Article

Rapid H{C}-Resolved Diffusion and Spin-Relaxation Measurements by NMR Spectroscopy

Christian A. Steinbeck, and Bradley F. Chmelka

J. Am. Chem. Soc., **2005**, 127 (33), 11624-11635• DOI: 10.1021/ja0439064 • Publication Date (Web): 29 July 2005

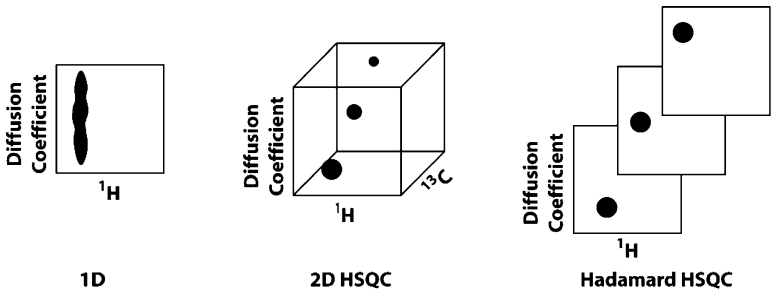

More About This Article

Additional resources and features associated with this article are available within the HTML version:

- Supporting Information
- Links to the 2 articles that cite this article, as of the time of this article download
- Access to high resolution figures
- Links to articles and content related to this article
- Copyright permission to reproduce figures and/or text from this article

View the Full Text HTML

J|A|C|S
ARTICLES
Published on Web 07/29/2005

Rapid $^{1}H\{^{13}C\}$-Resolved Diffusion and Spin-Relaxation Measurements by NMR Spectroscopy

Christian A. Steinbeck and Bradley F. Chmelka*

Contribution from the Department of Chemical Engineering, University of California, Santa Barbara, California 93106

Received October 6, 2004; E-mail: bradc@engineering.ucsb.edu

Abstract: Hadamard-encoded heteronuclear-resolved NMR diffusion and relaxation measurements allow overlapping signal decays to be resolved with substantially shorter measuring times than are generally associated with 2D heteronuclear cross-correlation experiments. Overall measuring time requirements can be reduced by approximately an order of magnitude, compared to typical 2D heteronuclear single-quantum correlation-resolved diffusion or relaxation measurements. Specifically, in cases where chemical shift correlation information provides enhanced spectral resolution, the use of Hadamard encoding can be used to overcome uniqueness challenges that are associated with the analysis of concurrent dynamic processes and the extraction of time constants from overlapping exponential signal decays. This leads to substantially improved resolution of similar time constants than can be achieved solely through the use of postacquisition processing techniques. In the ideal case of complete spectral separation of the signal decays, the usual constraint that time constants must be sufficiently different to resolve by exponential analysis can be circumvented entirely. Hadamard-based pulse sequences have been used to determine $^{1}H\{^{13}C\}$-resolved diffusion coefficients and spin-relaxation time constants for the chemically similar components of an aqueous solution of ethanol, glycerol, and poly(ethylene glycol), and a dye-containing block-copolymer solution, which exhibit significant spectral overlap in their ^{1}H NMR spectra.

Introduction

The measurement of diffusion coefficients and relaxation rates by nuclear magnetic resonance (NMR) spectroscopy can provide important insights into the dynamics of molecular processes over substantially different time and length scales.[1] For example, information on molecular rotation and intermolecular motions with picosecond to nanosecond time scales can be obtained from NMR relaxation rates.[2−6] By comparison, measurements of self-diffusion coefficients[7−10] are sensitive to longer range molecular mobilities and interactions on the order of milliseconds to seconds. In addition, diffusion measurements can be used to distinguish different molecular species and complexes in solution, a concept first introduced by Stilbs as "Size-Resolved NMR Spectroscopy"[11] and later extended by Morris and Johnson as "Diffusion Ordered Spectroscopy (DOSY)".[12] Although the details of the corresponding experimental measurements are quite different, the subsequent data analyses are similar and face the same challenges and limitations. Foremost among these is the difficulty of extracting similar time constants from noisy data in the presence of spectral overlap. By reducing the spectral overlap without drastically increasing the experimental time, the Hadamard-encoding methodology described here leads to significant simplification of subsequent data analyses and allows similar time constants to be extracted unambiguously without the need for time-intensive 2D NMR measurements. Consequently, Hadamard-encoded NMR techniques can enhance greatly the speed and accuracy by which diffusion and spin-relaxation processes are resolved and quantitatively measured for chemically similar components in liquid solutions.

Many physical processes, including nuclear spin-relaxation and molecular self-diffusion as measured by pulsed-gradient NMR experiments, manifest exponential signal decays that can be described by first-order differential equations. In spectral regions with well resolved peaks from molecular species that are each associated with a well-defined environment (on the time scale of 1D NMR measurements), analyses of the data are straightforward: the corresponding time constants are determined from nonlinear least-squares fits of each decaying signal to a separate monoexponential function. In contrast, for spectral regions with significant peak overlap, observed signal decays may be the result of superpositions of several individual decays that are difficult to distinguish. In such cases, the extraction of the corresponding time constants becomes challenging and often uncertain for reasons of uniqueness: multiple sets of time

(1) Delpuech, J. J., Ed. *Dynamics of Solutions and Fluid Mixtures by NMR*; John Wiley & Sons: New York, 1995.
(2) Kowalewski, J. *Annu. Rep. NMR Spectrosc.* **1991**, *23*, 289−374.
(3) Kowalewski, J. *Annu. Rep. NMR Spectrosc.* **1989**, *22*, 307−414.
(4) Palmer, A. G. *Annu. Rev. Biophys. Biomol. Struct.* **2001**, *30*, 129−155.
(5) Ishima, R.; Torchia, D. A. *Nat. Struct. Biol.* **2000**, *7*, 740−743.
(6) Kay, L. E. *Nat. Struct. Biol.* **1998**, *5*, 513−517.
(7) Johnson, C. S. *Prog. Nucl. Magn. Reson. Spectrosc.* **1999**, *34*, 203−256.
(8) Price, W. S. *Concepts Magn. Reson.* **1997**, *9*, 299−336.
(9) Price, W. S. *Concepts Magn. Reson.* **1998**, *10*, 197−237.
(10) Stilbs, P. *Prog. Nucl. Magn. Reson. Spectrosc.* **1987**, *19*, 1−45.
(11) Stilbs, P. *Anal. Chem.* **1981**, *53*, 2135−2137.
(12) Morris, K. F.; Johnson, C. S. *J. Am. Chem. Soc.* **1992**, *114*, 3139−3141.

10.1021/ja0439064 CCC: $30.25

constants may exist, all of which may fit the decay data equally well. This situation is made still more difficult when the number of contributing components is also unknown. For example, Lanczos showed that a biexponential decay could be reproduced to within less than one percent by a sum of three exponentials with significantly different time constants and initial amplitudes.[13] These difficulties arise because exponential functions are not orthogonal. As a consequence, the deviation of a numerical fit from the experimental data due to an incorrect fitting parameter can be compensated by the adjustment of one or more other parameters. The problem is exacerbated as the number of components in the observed decay increases and becomes even more complicated in the presence of experimental noise.[14] For example, it has been shown that, for a two-component biexponential decay with a signal-to-noise ratio (SNR) of 10^3 (a value rarely exceeded in NMR measurements), the corresponding time constants need to differ by at least a factor of 2 to be reliably determined using a nonlinear least-squares fit.[15] By increasing the number of components to three, the required separation increases to a factor of 3.5. A reduction in the SNR to 10^2 further increases the required separation to a factor of 10 for a three-component decay. Consequently, the extraction of an often unknown number of time constants from experimental data is challenging, even for data sets exhibiting high signal-to-noise ratios.

Much effort has therefore been focused on improving postacquisition data processing and on extending capabilities for resolving different time constants from overlapping signals, while circumventing the need for precise knowledge of the number of components. A number of such processing approaches are described in an excellent review by Istratov and Vyvenko[16] to which the reader is referred for their detailed discussion and comparison. The selection of a preferred data-processing method depends on a number of factors, including the signal-to-noise level, the number of exponentially decaying components, as well as the similarity of the time constants. Independent of the processing technique used, however, there exist inherent uniqueness difficulties and limitations in the temporal resolution achievable (i.e., the ratio of the time constants of two concurrent dynamic processes that can be resolved from a single multiexponential decay curve), which depend strongly on the signal-to-noise ratio of the measured decay.

In many cases, it is possible to improve temporal resolution by resolving overlapping signals spectroscopically, for example, by incorporating additional chemical shift information from multidimensional homonuclear or heteronuclear correlation experiments. Such an approach can resolve, in two or more frequency dimensions, NMR resonances that overlap in 1D measurements. Separate signal decay curves can subsequently be obtained for each resolved resonance, and single-exponential analyses can be used to yield unambiguous values for the corresponding time constants. In cases where the application of multidimensional experiments is not sufficient to resolve completely all overlapping resonances, the number of components associated with the observed signal decays may nevertheless be significantly reduced. Subsequent data processing can yield more reliable estimates of the time constants of interest than possible from the poorly resolved decays associated with the strongly overlapping signals obtained from 1D experiments. This approach has, for example, been used to determine the self-diffusivities[17−21] of molecular species in solution mixtures of similar components with enhanced spectral and temporal resolution. However, the additional resolution obtained by relying on multidimensional NMR methods comes with the disadvantage of dramatically increased experimental measurement times. Depending on the resolution required in the indirect dimension, measuring times may increase 10- to 1000-fold, which in many cases makes such an approach infeasible. This is especially true for systems that undergo changes on the time scales of such long multidimensional experiments.

Several experimental approaches have recently been demonstrated that allow faster acquisition of multidimensional NMR spectra. Frydman et al.,[22,23] for example, used spatially selective NMR excitation and detection to separate a sample into a series of subensemble regions. Instead of incrementing the evolution time in a series of independent experiments, as typically done in 2D NMR spectroscopy, each of these subensembles could then be used to encode information for a different evolution time and a full 2D spectrum effectively acquired in a single scan. Because of the small sample volume of each of these subensembles, this approach is especially useful for concentrated samples.

By comparison, Hadamard-encoded NMR spectroscopy[24−37] represents a conceptually different approach, which can be useful even for more dilute solutions. In Hadamard NMR, the evolution time in the indirect dimension is replaced by phase-encoded multisite selective excitation, so that the experimental time is effectively focused only on signal-containing spectral regions, instead of acquiring a complete spectrum in the indirect dimension. This approach has been used previously to investigate a number of dynamic processes. For example, the proton-deuteron exchange kinetics in backbone amide groups in the

(13) Lanczos, C. *Applied Analysis*; Prentice Hall: Englewood Cliffs, NJ, 1959.
(14) Bertero, M.; Boccacci, P.; Pike, E. R. *Proc. R. Soc. London* **1982**, *383*, 15−29.
(15) Clayden, N. J.; Hesler, B. D. *J. Magn. Reson.* **1992**, *98*, 271−282.
(16) Istratov, A. A.; Vyvenko, O. F. *Rev. Sci. Instrum.* **1999**, *70*, 1233−1257.
(17) Buevich, A. V.; Baum, J. *J. Am. Chem. Soc.* **2002**, *124*, 7156−7162.
(18) Williamson, R. T.; Chapin, E. L.; Carr, A. W.; Gilbert, J. R.; Graupner, P. R.; Lewer, P.; McKamey, P.; Carney, J. R.; Gerwick, W. H. *Org. Lett.* **2000**, *2*, 289−292.
(19) Parkinson, J. A.; Sun, H. Z.; Sadler, P. J. *Chem. Commun.* **1998**, 881−882.
(20) Barjat, H.; Morris, G. A.; Swanson, A. G. *J. Magn. Reson.* **1998**, *131*, 131−138.
(21) Steinbeck, C. A.; Hedin, N.; Chmelka, B. F. *Langmuir* **2004**, *20*, 10399−10412.
(22) Frydman, L.; Lupulescu, A.; Scherf, T. *J. Am. Chem. Soc.* **2003**, *125*, 9204−9217.
(23) Frydman, L.; Scherf, T.; Lupulescu, A. *Proc. Natl. Acad. Sci. U.S.A.* **2002**, *99*, 15858−15862.
(24) Blechta, V.; Freeman, R. *Chem. Phys. Lett.* **1993**, *215*, 341−346.
(25) Freeman, R.; Kupce, E. *J. Biomol. NMR* **2003**, *27*, 101−113.
(26) Krishnamurthy, K. *J. Magn. Reson.* **2001**, *153*, 144−150.
(27) Nishida, T.; Widmalm, G.; Sandor, P. *Magn. Reson. Chem.* **1996**, *34*, 377−382.
(28) Nishida, T.; Widmalm, G.; Sandor, P. *Magn. Reson. Chem.* **1995**, *33*, 596−599.
(29) Schraml, J.; vanHalbeek, H.; DeBruyn, A.; Contreras, R.; Maras, M.; Herdewijn, P. *Magn. Reson. Chem.* **1997**, *35*, 883−888.
(30) Van Melckebeke, N.; Simorre, J. P.; Brutscher, B. *J. Am. Chem. Soc.* **2004**, *126*, 9584−9591.
(31) vanHalbeek, H.; Schraml, J.; DeBruyn, A.; Contreras, R.; Maras, M.; Herdewijn, P. *Glycobiology* **1996**, *6*, 103−103.
(32) Bougault, C.; Feng, L. M.; Glushka, J.; Kupce, E.; Prestegard, J. H. *J. Biomol. NMR* **2004**, *28*, 385−390.
(33) Kupce, E.; Nishida, T.; Freeman, R. *Prog. Nucl. Magn. Reson. Spectrosc.* **2003**, *42*, 95−122.
(34) Kupce, E.; Freeman, R. *J. Magn. Reson.* **2003**, *163*, 56−63.
(35) Kupce, E.; Freeman, R. *J. Magn. Reson.* **2003**, *162*, 300−310.
(36) Kupce, E.; Freeman, R. *J. Magn. Reson.* **2003**, *162*, 158−165.
(37) Kupce, E.; Freeman, R. *J. Biomol. NMR* **2003**, *25*, 349−354.

protein ubiquitin have been probed by repeated acquisition of Hadamard-encoded $^1H\{^{15}N\}$ heteronuclear single-quantum correlation (HSQC) spectra.[32] In this study, chemical rate processes were quantified by monitoring reductions in ^1H signal intensity after diluting a fully protonated sample with D_2O to produce a system initially far from chemical equilibrium. Very recently, van Melckebeke et al. applied a Hadamard-encoded filter as a replacement for selective isotope labeling in $^1H\{^{13}C\}$ NOESY cross-relaxation experiments for the determination of methyl−methyl distances in amino acids.[30] The applicability of Hadamard encoding to heteronuclear-resolved relaxation measurements has also been suggested and proof-of-principle data have been reported in a recent review.[33]

Here, the incorporation of Hadamard encoding into NMR diffusion and spin-relaxation experiments is demonstrated to provide spectroscopically resolved transient signal decays for species with strongly overlapping 1D signals. The principal objectives are the unambiguous and rapid determination of diffusivities and relaxation times for a diverse range of complex solutions. These include especially those with components undergoing dynamic processes that are characterized by very similar time constants. Hadamard methods are shown to serve as a general basis for modifying a large number of other heteronuclear-resolved NMR experiments for the measurement of dynamic properties of complicated solution mixtures, including nonprotein systems and those in or far from chemical equilibrium. Enhanced spectral and temporal resolution are achievable in substantially shorter times than corresponding multidimensional experiments, while retaining the same information content. Measuring time requirements can be reduced by an order of magnitude, depending on the system under investigation, in this case an aqueous mixture of ethanol, glycerol, and poly(ethylene glycol) or a dye-containing block-copolymer solution. This allows for significantly more accurate and time-efficient determination of even very similar time constants associated with dynamic processes (e.g., self-diffusion coefficients or spin-relaxation times) in complicated solution mixtures than previously possible.

Theory and Background

The investigation of dynamic processes by NMR typically involves three steps: the preparation of an initial magnetization state, followed by a transient decay period, and subsequent detection of the resulting signal. During the preparation period, a specific and well-defined magnetization state is created by a series of radio frequency and possibly gradient pulses. The intensity of this state, I_0, serves as the initial intensity, after which the signal may become attenuated during the subsequent decay period. For diffusion measurements, the signal attenuation results from incomplete refocusing of magnetization at the end of the decay period.[8,38] In a typical stimulated-echo experiment,[9,39] the strength g of the applied gradient is varied and, from the resulting intensity decay (signal intensity as a function of the square of the gradient strength), the mean molecular self-diffusion coefficient can be determined by a monoexponential analysis. In such a case

$$\frac{I}{I_0^*} = \exp[-\gamma^2 g^2 \delta^2 (\Delta - \delta/3) D] \tag{3}$$

where I is the observed signal intensity of the refocused echo, I_0^* is the maximum signal intensity observed in the absence of the gradient pulses (including spin-relaxation losses), γ is the gyromagnetic ratio of the nucleus under investigation, g is the strength of the applied gradient pulse, δ is the duration of the gradient pulse, Δ is the diffusion time, and D is the self-diffusion coefficient. If signals overlap, the determination of diffusion coefficients from experimental data suffers from the general limitations associated with the exponential analyses discussed above.

For measurements of spin-relaxation times, by comparison, the signal attenuation during the decay period results not from incomplete refocusing in the presence of field gradients but rather from nuclear spin-relaxation processes. Typically, these are divided into two classes: longitudinal spin−lattice relaxation (T_1), which characterizes the return of the z-magnetization component in the direction of the applied field to thermal equilibrium, and transverse spin−spin relaxation (T_2), which characterizes the loss of phase coherence of magnetization in the xy plane normal to the applied field. Both of these processes can also be treated by monoexponential analyses:[40]

$$\frac{I}{I_0} = -a + b \exp(-\tau/T_i) \tag{4}$$

where I is the measured signal intensity, I_0 is the initial signal intensity measured in the absence of a decay period, a and b are constants that depend on the experiment being performed (e.g., $a = -1$, $b = 2$ for an inversion recovery experiment[40]), τ is the duration of the decay period during which spin relaxation is allowed to occur, and T_i is the spin-relaxation time constant (e.g., T_1 for an inversion recovery experiment). In a typical series of experiments, the duration of the decay time, τ, is varied, yielding an exponential decay in the measured signal intensity from which the relaxation time constant, T_i, is determined. In the presence of overlapping signals, such an analysis suffers from the aforementioned difficulties of uniquely extracting different time constants from the resulting signal decays, which are analogous to those previously described for the determination of diffusion coefficients.

As introduced above, one solution to the problem of overlapping signals is to modify the detection period to incorporate a multidimensional heteronuclear segment in order to spread and correlate NMR frequencies in more than one spectral dimension. For example, a $^1H\{^{13}C\}$ HSQC experiment correlates signals from ^{13}C moieties with directly bonded (J-coupled) protons, yielding 2D spectra in which correlated signal intensity is observed at the corresponding ^{13}C and ^1H chemical shifts. It is possible to circumvent the long measuring time requirements associated with such multidimensional correlation experiments by concentrating on those spectral regions that contain resonance signals. This is achieved by replacing the evolution time of a 2D experiment with pulses that selectively excite the resonances of interest. Multidimensional NMR techniques, however, also benefit from multiplexing; i.e., each time-domain data point that

(38) Stejskal, E. O.; Tanner, J. E. *J. Chem. Phys.* **1965**, *42*, 288−292.
(39) Tanner, J. E. *J. Chem. Phys.* **1970**, *52*, 2523−2526.
(40) Abragam, A. *The Principles of Nuclear Magnetic Resonance*; Clarendon Press: Oxford, 1961.

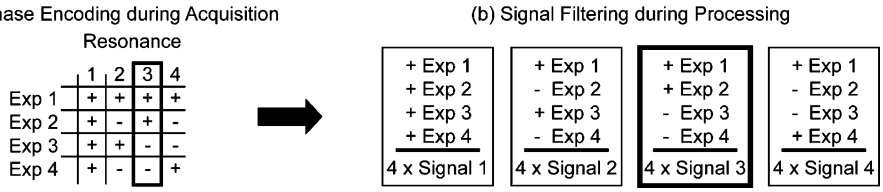

Figure 1. Phase-encoding and signal-filtering summaries of Hadamard-encoded NMR spectroscopy for an arbitrary sample containing four distinctly resolved resonances. (a) During signal acquisition the various resonances are selectively phase-encoded (positive or negative), according to the matrix shown. For the case of four different resonances, the experiment is repeated four times (Exp 1, 2, 3, and 4) with varying phase encoding. (b) During processing, the signals corresponding to each of the four resonances are separated by addition or subtraction of the free-induction decays obtained in each of the four experiments. The elements outlined in bold are discussed specifically in the text.

is collected in the indirect dimension contains information about each point in the frequency domain. To regain this multiplexing benefit, it is necessary to irradiate a sample at several different frequencies simultaneously (multiplexing) and later extract the individual contributions from the observed signal. As first demonstrated by Golay[41] in infrared spectroscopy, it is possible to use Hadamard encoding and decoding to achieve the separation of the individual signal contributions. The introduction of Fourier transform NMR[42] (FT-NMR), which is inherently a multiplexing technique, superseded efforts by Anderson[43] to achieve similar sensitivity advantages in NMR. In many cases, and especially in multidimensional NMR, the use of selective excitation and Hadamard encoding (as opposed to the broadband excitation used in FT-NMR) can however be beneficial, as illustrated in a recent comprehensive review by Kupce et al.[33]

By applying the Hadamard methodology, filtered NMR spectra can be obtained by judicious processing (addition and subtraction) of the free-induction decays (FIDs) corresponding to a sufficient number of experiments. In general, 4*m* such experiments are required, where *m* is chosen such that 4*m* is the smallest multiple of 4 that is greater than or equal to the number of signals to be resolved.[24,34,44,45] For example, four separate Hadamard experiments must be performed with different phase encodings for a system containing four distinct resonances in order to obtain selectively filtered spectra for each of the individual resonances. The appropriate phase encodings and postacquisition processing are illustrated schematically in Figure 1a and b, respectively. For example, the signal corresponding to the third resonance would be phase-encoded [Figure 1a, outlined in bold] to be positive in the first and second experiments and negative in the third and fourth experiments. As depicted in the bolded box of Figure 1b, a corresponding filtered spectrum would then be obtained by adding together the phase-encoded FIDs acquired in experiments 1 and 2 and subtracting those acquired in experiments 3 and 4. This combination of additions and subtractions, leads to a filtered 1D NMR spectrum in which the signal intensity of the third resonance is four times that obtained in each individual experiment, while the contributions from the remaining resonances have been canceled. Different, but analogous, addition and subtraction combinations of the same Hadamard-phase-encoded FIDs can be used to obtain filtered spectra for each of the remaining resonances, as similarly indicated in Figure 1b. By implementing a Hadamard-encoded heteronuclear component in the detection period of self-diffusion and spin-relaxation experiments, it is possible to separate signals that overlap when using a conventional 1D detection scheme. This has the benefit of significantly improving the temporal resolution of similar time constants, while avoiding the long experimental times of 2D measurements.

Experimental Section

Ethanol [CH_3CH_2OH], glycerol [$HOCH_2-CHOH-CH_2OH$], poly(ethylene glycol) [$(-OCH_2CH_2-)_n$ with $n_{average} = 80$], and D_2O were used as received from Sigma-Aldrich (St. Louis, MO). Two solution-state samples were used in the first part of this study: (1) 10 wt % glycerol in D_2O and (2) 5 wt % ethanol, 10 wt % glycerol, and 2 wt % poly(ethylene glycol) in D_2O. A 400 μL aliquot of each sample was placed in separate 5 mm NMR tubes and analyzed using a Bruker AVANCE 500 spectrometer operating at 500.13 MHz for ^1H and 125.76 MHz for ^{13}C at room temperature (298 K, calibrated using methanol). Experiments were performed using a triple-axis gradient probehead with maximum gradient strengths of 6.65 G/mm in the *z*-direction and 5.01 G/mm in the *x*- and *y*-directions (calibrated using the diffusion coefficient of water at 298 K).

Gradient-selected 2D $^1H\{^{13}C\}$ HSQC experiments[46,47] consisted of 2 scans for each of 128 data points in the indirectly detected ^{13}C dimension and 8096 data points in the directly detected ^1H dimension. Globally optimized alternating-phase rectangular-pulse (GARP)[48] ^{13}C decoupling was applied with a field strength of 3 kHz during signal acquisition. The corresponding Hadamard-encoded experiments consisted of 4 scans for each of the 8 experiments necessary to resolve the five $^1H\{^{13}C\}$ resonances considered here, i.e., the $-CH_2OH$ and $-CH_3$ resonances of ethanol, the $-CH_2OH$ and $-CHOH-$ resonances of glycerol, and the $-OCH_2CH_2-$ resonances of poly(ethylene glycol). The selective inversion pulses were shifted laminar pulses[49] with Gaussian shapes and pulse lengths of 7 ms. Forward and reverse INEPT magnetization transfer periods, *d*, were used, corresponding to $1/(4J_{CH})$ with $J_{CH} = 145$ Hz.[50] GARP ^{13}C decoupling with a field strength of 3 kHz was applied for approximately 1.3 s during the acquisition period of the Hadamard-encoded experiments. In addition, WALTZ-16 ^1H decoupling[51] was applied with a field strength of 6 kHz during the selective ^{13}C pulses of the Hadamard sequences. To maintain the existing longitudinal spin order after selective inversion, the duration

(41) Golay, M. J. E. *J. Opt. Soc. Am.* **1949**, *39*, 437−444.
(42) Ernst, R. R.; Anderson, W. A. *Rev. Sci. Instrum.* **1965**, *36*, 1696−1706.
(43) Anderson, W. A. In *Encyclopedia of Nuclear Magnetic Resonance*; Grant, D. M., Harris, R. K., Eds.; Wiley: Chichester, UK; 1996; Vol. 1, pp 168−176.
(44) van Lint, J. H.; Wilson, R. M. *A Course in Combinatorics*; Cambridge University Press: New York, 1993.
(45) This is strictly true only up to a maximum matrix size of 428 × 428,[44] but in practice the use of Hadamard encoding is not efficient for such a large number of resonances. In addition Hadamard matrices of size 2 × 2 also exist.
(46) Willker, W.; Leibfritz, D.; Kerssebaum, R.; Bermel, W. *Magn. Reson. Chem.* **1993**, *31*, 287−292.
(47) Vuister, G. W.; Boelens, R.; Kaptein, R.; Hurd, R. E.; John, B.; van Zijl, P. C. M. *J. Am. Chem. Soc.* **1991**, *113*, 9688−9690.
(48) Shaka, A. J.; Barker, P. B.; Freeman, R. *J. Magn. Reson.* **1985**, *64*, 547−552.
(49) Shifted laminar pulses are essentially linear superpositions of individual selective pulses in which the frequency offset of the individual pulses is achieved through phase modulation.
(50) An average value was used for the *J*-coupling, resulting in efficient magnetization transfer for all of the proton-carbon pairs investigated.
(51) Shaka, A. J.; Keeler, J.; Frenkiel, T.; Freeman, R. *J. Magn. Reson.* **1983**, *52*, 335−338.

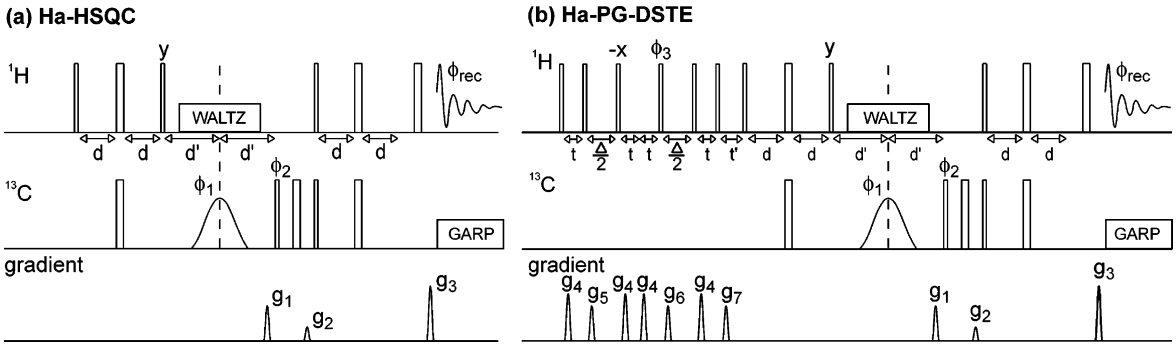

Figure 2. Schematic diagrams of pulse sequences for (a) a Hadamard-encoded gradient-selected heteronuclear single-quantum correlation (Ha-HSQC) experiment and (b) a pulsed-gradient double-stimulated-echo experiment with Ha-HSQC detection (Ha-PG-DSTE). Wider and narrower pulse features correspond to π and $\pi/2$ pulses, respectively, labeled boxes correspond to decoupling periods, and Gaussian shapes indicate shifted laminar selective pulses used for Hadamard encoding. The bottom-most line in each pulse program corresponds to the gradient channel. The diffusion time in the PG-DSTE sequences is abbreviated as Δ, and the transfer time in the INEPT blocks is abbreviated as d and set to $1/(4J_{CH})$. The selective laminar ^{13}C pulse and the WALTZ ^1H decoupling are centered between the preceding ^1H and the subsequent ^{13}C $\pi/2$ pulses. The delay $2d'$ was chosen to be just long enough to include the selective pulse and the spoil gradient g_1 (including a gradient recovery delay), while ensuring that an integer number of WALTZ-16 cycles was carried out. For the Ha-PG-DSTE experiment, the delay t was chosen to accommodate the diffusion gradients (including a gradient recovery delay), and the eddy current delay t' was kept short (10 ms) to minimize relaxation losses. All phases are x unless otherwise specified. The following phase cycles were employed: (a) Ha-HSQC: $\phi_1 = (x)_2, (-x)_2$; $\phi_2 = x, -x$; $\phi_{rec} = x, -x, -x, x$; (b) Ha-PG-DSTE: $\phi_1 = (x)_4, (-x)_4$; $\phi_2 = x, -x$; $\phi_3 = (-x)_2, (x)_2$; $\phi_{rec} = x, -x, -x, x, -x, x, x, -x$. The following gradient strengths were used in the different experiments: (a) Ha-HSQC: spoil gradient $g_1 = 1.25$ ms at 4.35 G/mm, encoding gradient $g_2 = 1.00$ ms at 6.52 G/mm, decoding gradient $g_3 = 1.00$ ms at 1.63 G/mm ($g_2/g_3 = 4:1$). (b) Ha-PG-DSTE: g_1, g_2, g_3 as for Ha-HSQC, diffusion gradient $g_4 = 2.5$ ms with varying gradient strength, spoil gradient $g_5 = 1.0$ ms at 0.65 G/mm, spoil gradient $g_6 = 1.0$ ms at 0.75 G/mm, and spoil gradient g_7 at 1.05 G/mm.

of the ^1H decoupling period was chosen such that it contained only complete WALTZ-16 cycles.

Pulsed-gradient stimulated-echo diffusion experiments were performed using a diffusion time, Δ, of 200 ms with encoding and decoding gradients in the z-direction of duration $\delta = 2.5$ ms and gradient strengths varying from 0.13 G/mm to 6.32 G/mm. All experimentally observed diffusion coefficients were normalized to the diffusion coefficient of water, which was determined from the proton resonance associated with residual non-perdeuterated water (HDO, H_2O). Heteronuclear-resolved ^{13}C T_1 relaxation times were measured by using a pulse sequence proposed by Jin et al.[52] In this pulse sequence, a sandwich of four $\pi/2$ pulses and four gradient pulses is repeated during the relaxation time to remove the effects of cross-correlations. For these ^{13}C T_1 measurements, the relaxation times were varied between 200 ms and 10 s with ^1H π pulses applied every 10 ms. Recycle delays (10 s) were used between successive scans. For the directly excited/detected ^{13}C relaxation measurements, WALTZ-16 ^1H decoupling with a field strength of 6 kHz was applied during signal acquisition. In validating the applicability of the Hadamard-encoded HSQC-resolved ^{13}C T_2 relaxation measurements, ^{13}C refocusing pulses during the CPMG period were separated by $2\tau = 900$ μs, and ^1H π-pulses were applied every 7.20 ms to remove cross-correlation effects.[53] For the ^1H T_2 measurements, the refocusing ^1H π-pulses were separated by 1.40 ms.

For the investigation of the solution-state interactions between charged porphyrin dye molecules and block copolymers, a 10 mM aqueous solution of both *tetra*(4-sulfonatophenyl)-porphyrin ($TPPS_4$, Frontier Scientific) and the poly(ethylene oxide)-poly(propylene oxide)-poly(ethylene oxide) triblock copolymer EO_{20}-PO_{70}-EO_{20} (Pluronic P123, BASF) was prepared in D_2O. The pH (here, reflecting the concentration of deuterons, rather than protons) was adjusted to 11 through the addition of sodium deuterioxide (NaOD 99.9%, Sigma Aldrich). A diffusion time $\Delta = 200$ ms was used with diffusion encoding/decoding gradient pulses of length $\delta = 7$ ms for both the Hadamard-encoded, as well as the full quasi-3D HSQC, diffusion measurements.

Results and Discussion

Hadamard-Encoded HSQC (Ha-HSQC). The use of Hadamard encoding allows otherwise overlapping resonances to be resolved without the long measuring times that are inherent in typical heteronuclear-resolved diffusion and spin-relaxation measurements. A Hadamard-encoded version of the heteronuclear single-quantum correlation (HSQC) experiment was used here and is shown in Figure 2a. It is based on a pulse sequence described by Kupce and Freeman[34] but modified to be less prone to pulse miscalibrations and other experimental artifacts. The pulse sequence consists of an initial INEPT[54] (Insensitive Nuclei Enhanced through Polarization Transfer) block to transfer magnetization from ^1H to ^{13}C. In contrast to a regular 2D HSQC experiment, only longitudinal spin order is necessary for labeling ^{13}C magnetization with selective pulses. For this reason, the last ^{13}C $\pi/2$ pulse of the full INEPT block could be omitted. After Hadamard phase-encoding, the ^{13}C moieties are labeled with a gradient pulse, by rotating the ^{13}C magnetization into the transverse plane using the ^{13}C $\pi/2$ pulse immediately following the selective pulse. The inclusion of such gradient labeling allows for clean selection of signals from those ^1H moieties that are directly bonded to ^{13}C atoms and also leads to a reduction in the number of phase cycling steps. Following the gradient encoding, the magnetization is transferred to covalently bonded protons by a reverse INEPT block, decoded with a second gradient pulse, and finally detected. In addition, a simple phase cycle of the basic Hadamard phase labeling was implemented to eliminate artifacts arising from imperfect selective inversion pulses. This was achieved by performing the Hadamard experiment twice, once with the phase encoding specified by the original Hadamard matrix and once with its inverse (i.e., changing positive phase encoding to negative and vice-versa). By adding the result of the first and second sets of Hadamard experiments, artifacts that would arise from imperfect

(52) Jin, C. W.; Prompers, J. J.; Bruschweiler, R. *J. Biomol. NMR* **2003**, *26*, 241−247.
(53) Kay, L. E.; Nicholson, L. K.; Delaglio, F.; Bax, A.; Torchia, D. A. *J. Magn. Reson.* **1992**, *97*, 359−375.
(54) Morris, G. A.; Freeman, R. *J. Am. Chem. Soc.* **1979**, *101*, 760−762.

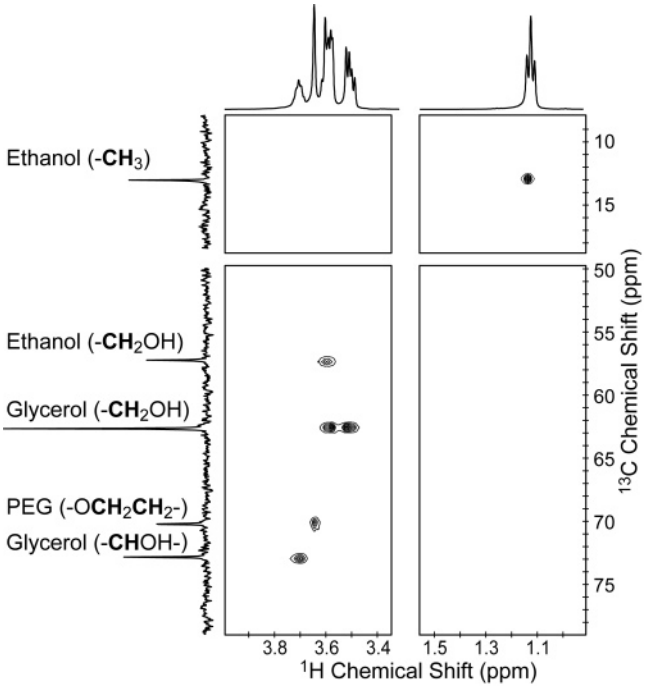

Figure 3. 2D ^{1}H{^{13}C} heteronuclear single-quantum correlation (HSQC) NMR spectrum obtained for a mixture of 5 wt % ethanol, 10 wt % glycerol, and 2 wt % poly(ethylene glycol) in D_2O at 298 K. The accompanying 1D ^{1}H and ^{13}C solution-state spectra shown were acquired in separate one-pulse experiments. All resonances are clearly resolved in the 2D HSQC spectrum, whereas significant overlap is observed among the protonated moieties of ethanol and glycerol in the 1D ^{1}H spectrum.

inversion are canceled, similar to the $(x, -x)$ phase cycling of π pulses in standard experiments.

The validity of using Hadamard encoding to obtain ^{1}H{^{13}C}-resolved heteronuclear single-quantum coherence (HSQC) NMR spectra is illustrated in Figures 3 and 4 for an aqueous solution of 5 wt % ethanol, 10 wt % glycerol, and 2 wt % poly(ethylene glycol) at 298 K. Figure 3 shows a full 2D ^{1}H{^{13}C} HSQC spectrum obtained using 2 scans and 128 points in the indirectly measured ^{13}C dimension, along with one-pulse 1D solution-state ^{1}H and ^{13}C spectra. In contrast to the 1D ^{1}H spectrum, all the resonances are well-resolved in the 2D ^{1}H{^{13}C} HSQC spectrum and can be assigned based on their ^{1}H and ^{13}C chemical shifts. Ethanol gives rise to two distinct signals, one corresponding to the $-\mathbf{C}\mathbf{H}_3$ group at 13 ppm ^{13}C and 1.10 ppm ^{1}H and one at 57 ppm ^{13}C and 3.60 ppm ^{1}H corresponding to the $-\mathbf{C}\mathbf{H}_2$OH groups. A single signal is observed for poly(ethylene glycol) at 71 ppm ^{13}C and 3.65 ppm ^{1}H corresponding to the $-\mathrm{O}\mathbf{C}\mathbf{H}_2\mathbf{C}\mathbf{H}_2-$ moieties. The glycerol species give rise to two distinct signals, one at 73 ppm ^{13}C and 3.70 ppm ^{1}H corresponding to the $-\mathbf{C}\mathbf{H}$OH$-$ moieties and a pair at 63 ppm ^{13}C and 3.60 and 3.52 ppm ^{1}H corresponding to the $-\mathbf{C}\mathbf{H}_2$OH groups. Figure 4 shows two representative ^{1}H spectra that were obtained with similar signal-to-noise ratios and resolution for the same mixture by using the Hadamard-encoded pulse sequence of Figure 2(a) and from corresponding slices extracted from the 2D ^{1}H{^{13}C} HSQC data set. To achieve comparable results with the Hadamard technique, eight separate experiments consisting of four scans each were performed, representing time savings of a factor of 8 ([128·2]/[8·4] = 8) for this particular measurement.[55]

Because of the inherent differences between Hadamard-encoded and standard multidimensional NMR spectroscopy methods, the time savings that can be realized depend on the experimental system under investigation, but it is possible to obtain a first estimate by considering the relevant experimental parameters. In a standard two-dimensional (2D) NMR experiment, the minimum number of points, n_P, required in the indirect dimension can be estimated from the sweep width, S_W, and the separation of the closest signals that need to be resolved, R:

$$n_P = \frac{2S_W}{R} \tag{5}$$

In practice, one typically needs to acquire a factor of 2 or even a factor of 4 more points to obtain well-resolved peaks. The use of zero-filling or linear prediction may also promote better resolution, because the frequency spacing of the Fourier transformed spectrum is inversely proportional to the number of data points.

In Hadamard-encoded NMR spectroscopy, on the other hand, one does not generate free-induction decays in the indirect dimension, so that the number of required scans consequently does not depend on the sweep width nor the separation of signals.[37] Rather, selective excitation or inversion allows the measurement time to be concentrated on signal-containing frequency regions, instead of acquiring over the entire frequency domain in both dimensions. The spectral resolution in the Hadamard dimension (corresponding to the indirect dimension of a 2D experiment) is approximately inversely proportional to the length of the selective excitation or inversion pulse.[56] Increasing the spectral resolution therefore affects the length of the experiments only indirectly, because possible relaxation losses during the longer selective pulse must be compensated for by accumulating a greater number of scans. This means that, regardless of the sweep width and the required spectral resolution, the total time of a Hadamard-encoded NMR experiment is approximately proportional to the size, n_H, of the Hadamard matrix used, where n_H is chosen to be the smallest multiple of 4 larger than the number of resonances that need to be resolved.[45] The relative time savings that can be realized by using Hadamard encoding can thus be estimated as follows:

$$\frac{t_{2D}}{t_{\mathrm{Hadamard}}} \propto \frac{2(S_W/R)_{2D}}{n_H} \tag{6}$$

For the example described above, with S_W = 8000 Hz, R = 400 Hz, and n_H = 8, the time savings were estimated with eq 6 to be approximately a factor of 5, in good agreement with those realized experimentally above. Hadamard-encoded HSQC thus allows for significantly shorter measuring times to be used compared to full 2D experiments, while yielding comparable signal-to-noise ratios and resolution.

Hadamard-Encoded, ^{1}H{^{13}C}-Resolved Diffusion Measurements (Ha-PG-DSTE). Recently, the HSQC technique has been used, in combination with pulsed-gradient methods, to resolve and measure the diffusivities of species with strongly overlapping 1D resonances.[17−21] By incorporating Hadamard encoding into the HSQC sequence, such heteronuclear-resolved diffusion measurements can be conducted in substantially shorter

(55) It is possible to obtain substantially better resolution and cleaner selection by increasing the number of scans and incorporating a more extensive phase cycling, but for illustration purposes the smallest number of experiments necessary to achieve satisfactory results was chosen here.

(56) Freeman, R. *Prog. Nucl. Magn. Reson. Spectrosc.* **1998**, *32*, 59−106.

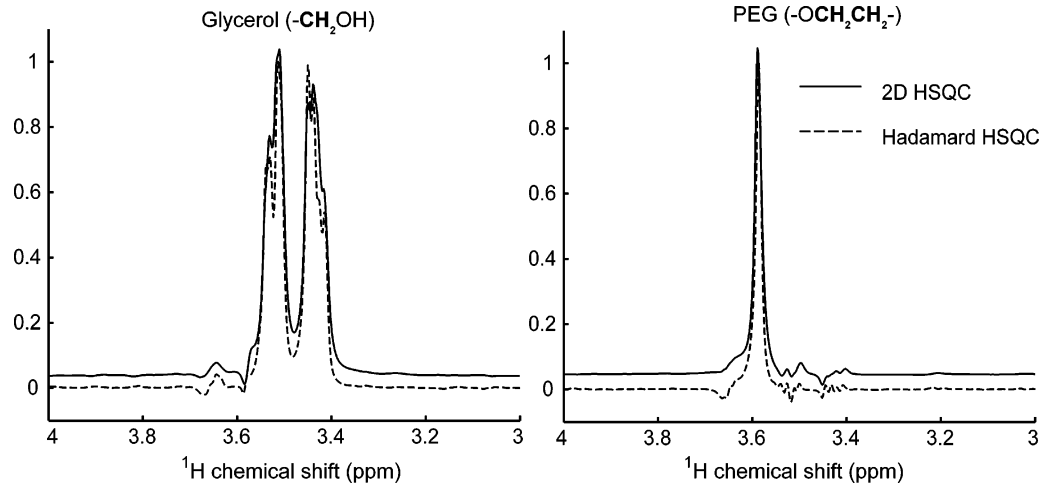

Figure 4. Comparison of slices obtained from a full 2D $^1H\{^{13}C\}$ HSQC experiment with spectra obtained from the Hadamard-encoded HSQC experiment. The results from the full 2D experiment are vertically offset from 0 to facilitate comparison. The sample consisted of a mixture of 5 wt % ethanol, 10 wt % glycerol, and 2 wt % poly(ethylene glycol) in D_2O at 298 K. For the experimental conditions used (2D HSQC: 2 scans, 128 points in the indirect dimension; 1D Ha-HSQC: 4 scans, 8 experiments), similar resolution and signal-to-noise ratios were obtained. The small artifacts that still remain in both experiments could be alleviated by extended phase cycles and correspondingly longer measuring times; the objective here was to illustrate the minimum experimental time required for a Hadamard measurement to yield comparable resolution and sensitivity to a full 2D HSQC experiment, which required 8 times longer to acquire.

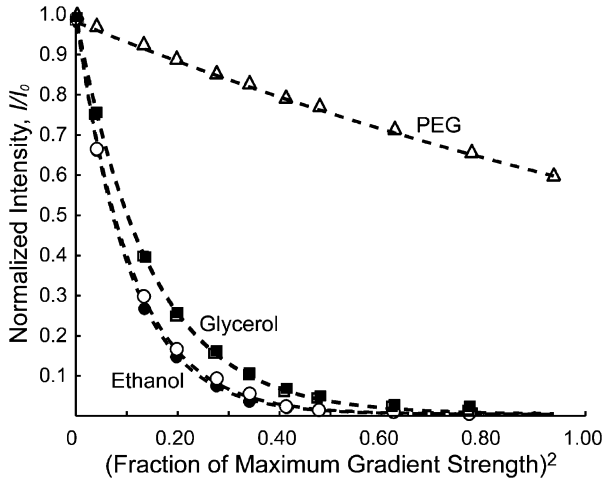

Figure 5. Signal decays obtained by varying the strength of the applied gradients in a pulsed-gradient double-stimulated-echo (Ha-PG-DSTE) diffusion measurement using a Hadamard-encoded heteronuclear single-quantum correlation block during the acquisition [Figure 2b]. The sample consisted of a mixture of 5 wt % ethanol, 10 wt % glycerol, and 2 wt % poly(ethylene glycol) in D_2O at 298 K. Monoexponential signal decays are observed for all resonances: poly(ethylene glycol) $-O\mathbf{CH_2CH_2}-$ (△), glycerol $-\mathbf{CH}OH-$ (■), and $-\mathbf{CH_2}OH$ (□), as well as ethanol $-\mathbf{CH_3}$ (●) and $-\mathbf{CH_2}OH$ (○). The decays observed for the overlapping $-\mathbf{CH_2}OH$ glycerol and ethanol resonances (empty symbols) agree well with those observed for the corresponding nonoverlapping resonances (solid symbols). All observed decays were fitted with single exponential decays, which are shown as dashed lines.

times. The Hadamard-encoded HSQC sequence discussed above [Figure 2a] was modified by replacing the first $\pi/2$ ^1H pulse in the Ha-HSQC sequence with a pulsed-gradient double-stimulated-echo (PG-DSTE) block, yielding the Ha-PG-DSTE sequence shown in Figure 2b. In this way, the modulated ^1H signal intensity produced by the PG-DSTE sequence serves as the initial intensity for the Ha-HSQC sequence. The ability to separate spectroscopically the signal decays using the Ha-PG-DSTE pulse sequence is demonstrated in Figure 5 for an aqueous solution of 5 wt % ethanol, 10 wt % glycerol, and 2 wt % poly(ethylene glycol) at 298 K. Monoexponential decays are observed for each of the correlated $^1H\{^{13}C\}$ signals associated with the five spectroscopically distinct sites, the resulting fits for which are shown as dashed lines in Figure 5. Ethanol and glycerol each give rise to two distinct signals in the correlated $^1H\{^{13}C\}$ experiments, corresponding to the $-\mathbf{CH_3}$ and $-\mathbf{CH_2}OH$ groups of ethanol and the $-\mathbf{CH_2}OH$ and $-\mathbf{CH}OH-$ groups of glycerol. In both cases, the same diffusion coefficients were determined from the separate decays of each of the two resonances for ethanol and glycerol. Consistent with the relative molecular weights of the species and their hydrogen-bonding capacities, ethanol showed the larger diffusivity, $D^{CH_3}_{EtOH}/D^{298}_{water} = 0.352 \pm 0.005$ and $D^{CH_2OH}_{EtOH}/D^{298}_{water} = 0.347 \pm 0.008$, while glycerol diffused more slowly, $D^{CH_2OH}_{glyc}/D^{298}_{water} = 0.258 \pm 0.003$ and $D^{CHOH}_{glyc}/D^{298}_{water} = 0.256 \pm 0.004$. Poly(ethylene glycol) exhibited the smallest diffusion coefficient, $D^{OCH_2}_{PEG}/D^{298}_{water} = 0.0187 \pm 0.0005$, consistent with its macromolecular character.

The suitability of the Ha-PG-DSTE pulse sequence and the validity of the results were verified by comparing the diffusion coefficients above with those measured for the same mixture in separate 1D ^1H experiments. For both ethanol and glycerol, at least one of their proton resonances is essentially free from overlap in a conventional 1D ^1H PG-DSTE experiment, so that self-diffusion coefficients can be independently determined from monoexponential fits to the decays of the resolved signals. The self-diffusion coefficients obtained separately from these measurements, $D^{CH_3}_{EtOH}/D^{298}_{water} = 0.350 \pm 0.006$ for the ethanol $-\mathbf{CH_3}$ moieties and $D^{CHOH}_{glyc}/D^{298}_{water} = 0.259 \pm 0.005$ for the glycerol $-\mathbf{CH}OH-$ moieties, correspond closely to those obtained from the Hadamard-encoded experiments, confirming the validity of the Hadamard approach. Compared to a full quasi-3D $^1H\{^{13}C\}$ HSQC-PG-DSTE experiment, the Hadamard-encoded measurement could be achieved in one-eighth ($^1/_8$) of the time.

For both Hadamard-encoded and HSQC-encoded diffusion measurements, it is necessary to avoid complications that may arise from intense rf-power input. For example, in both cases, it is often desirable to apply high power ^{13}C decoupling during signal acquisition, which can lead to local heating that may

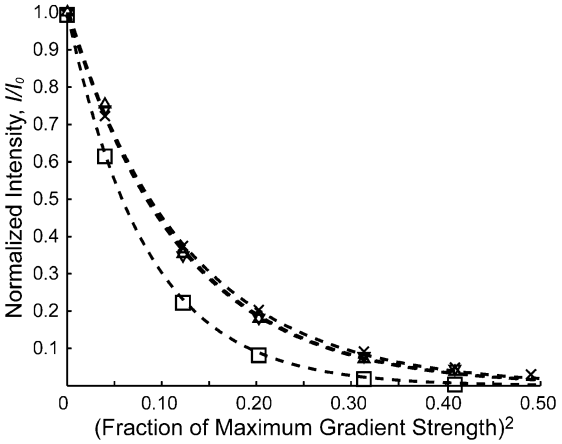

Figure 6. Comparison of the ^{1}H signal decays observed for various NMR diffusion measurements for a 10 wt % solution of glycerol in D_2O at 298 K. Data for conventional single-stimulated-echo experiments (no decoupling) with a recycle delay of 3 s are shown (×), along with data obtained from Hadamard-encoded heteronuclear single-quantum correlation (Ha-PG-STE) experiments with recycle delays of 30 s (▽) and 3 s (□), and data obtained using a double-stimulated-echo version of the Hadamard technique with a recycle delay of 3 s (△). Measurements using the Ha-PG-STE sequence showed significant deviations from the other measurements, unless long recycle delays (≥30 s) were used. When using such long recycle delays or employing the double-stimulated-echo Ha-PG-DSTE sequence, the resulting decay curves agree well with those obtained in the absence of decoupling. All observed decays were fitted with single exponential decays, which are shown as dashed lines.

produce undesirable temperature gradients within the sample.[57−59] Such thermal gradients may result from spatially heterogeneous heating during decoupling arising from rf-field inhomogeneities or from the associated cooling that is required to maintain the sample at a constant macroscopic temperature. These temperature gradients may in turn give rise to convection currents that could interfere strongly with the diffusion measurements;[60,61] when present, they will in general produce convection-induced dephasing that leads to the measurement of erroneously large apparent "diffusivity" values. Whether such factors are important under the conditions of the Hadamard-encoded diffusion measurements considered here was examined for a separate 10 wt % solution of glycerol at room temperature (298 K).

Figure 6 shows the results for several different Hadamard-encoded ^{1}H{^{13}C} diffusion measurements in which ^{1}H signals were recorded with ^{13}C decoupling during signal acquisition. Results for single- and double-stimulated-echo pulse sequences with different relaxation delays are compared to those obtained by using a 1D ^{1}H single-stimulated-echo pulse sequence in the absence of decoupling, which is expected to provide ^{1}H signal decays that are free from convection effects and which therefore reflect the true self-diffusion behavior of the glycerol species in solution. Figure 6 shows that significantly different ^{1}H signal decays can be observed for an aqueous glycerol solution, depending on the length of the recycle delay between scans, whether decoupling is applied or whether a single- or double-stimulated-echo sequence is used. In the absence of decoupling, the use of a 1D ^{1}H *single*-stimulated-echo pulse sequence resulted in a single-exponential decay (×) for both ^{1}H resonances from which the diffusivity of glycerol was determined to be $D_{\mathrm{glyc}}^{\mathrm{1D-STE}}/D_{\mathrm{water}}^{298} = 0.301 \pm 0.006$ (this value is somewhat higher than the diffusivity measured for glycerol in the PEG-containing mixture above, consistent with the higher viscosity of the polymer solution). The application of a Hadamard-encoded *single*-stimulated-echo pulse sequence (Ha-PG-STE) under otherwise identical conditions, on the other hand, leads to a significantly faster signal decay (□) and therefore to a correspondingly larger apparent "diffusion" coefficient, $D_{\mathrm{glyc}}^{\mathrm{Ha-STE}}/D_{\mathrm{water}}^{298} = 0.457 \pm 0.005$. This much larger value reflects a convective contribution to species mobility in the sample as a consequence of sample heating produced by the higher power input required for the Hadamard pulse sequence. Nevertheless, by increasing the recycle delay times, t_R, to greater than 30 s (▽), the duty cycle is reduced and convection currents are allowed to dissipate between scans. Under these conditions a diffusion coefficient value is obtained using the Ha-PG-STE sequence, $D_{\mathrm{glyc}}^{\mathrm{Ha-STE}}/D_{\mathrm{water}}^{298} = 0.307 \pm 0.007$, that agrees well with that measured using the 1D STE experiment in the absence of convection (×). Alternatively, undesired influences from such fluid convection currents can be avoided independently of t_R by the use of a *double*-stimulated-echo (DSTE) sequence (△), which yielded an accurate value for the diffusion coefficient, $D_{\mathrm{glyc}}^{\mathrm{Ha-DSTE}}/D_{\mathrm{water}}^{298} = 0.309 \pm 0.008$. In the DSTE pulse sequence, the unwanted dephasing of magnetization resulting from convection during the first diffusion period is, to first-order, removed during the second diffusion period, independent of the recycle delay time (t_R) used. Consequently, there is good agreement between results obtained with the Hadamard-encoded *single*-echo pulse sequence using a recycle delay time of 30 s (▽), with the Hadamard-encoded *double*-echo pulse sequence (t_R = 3 s, △) and with the single-echo ^{1}H sequence without decoupling (×). In practice, the choice between the use of long recycle delays versus a double-stimulated-echo sequence depends on the relaxation properties of the sample under investigation. For samples with long relaxation times, i.e., comparable to the time required for convection currents to subside, the use of a single stimulated echo is likely to be preferred, because of the signal loss (∼50%) associated with the use of a second stimulated echo in the PG-DSTE sequence.[62]

The Hadamard-encoded PG-DSTE (*double*-stimulated-echo) experiment and the Hadamard-encoded PG-STE (*single*-stimulated-echo) experiment with a long recycle delay are thus both suitable for the determination of ^{1}H{^{13}C}-resolved molecular self-diffusion coefficients. They can be used to determine accurately and rapidly the diffusion coefficients for species that exhibit significant spectral overlap in a 1D ^{1}H NMR spectrum, but which yield resolved signals in a 2D heteronuclear ^{1}H{^{13}C} correlation experiment. This has been demonstrated for overlapping ethanol and glycerol ^{1}H resonances and requires a factor of 8 less time to achieve than the corresponding quasi-3D HSQC-PG-DSTE measurement. In the ideal case, the resultant resolved signal decays will be monoexponentials, and the resolution limit for the determination of diffusion coefficients from superimposed decay curves would be eliminated. For the ethanol−glycerol−poly(ethylene glycol) mixture examined here, this allowed the diffusion coefficients of poly(ethylene glycol),

(57) Jerschow, A. *J. Magn. Reson.* **2000**, *145*, 125−131.
(58) Wang, A. C.; Bax, A. *J. Biomol. NMR* **1993**, *3*, 715−720.
(59) Led, J. J.; Petersen, S. B. *J. Magn. Reson.* **1978**, *32*, 1−17.
(60) Jerschow, A.; Müller, N. *J. Magn. Reson.* **1997**, *125*, 372−375.
(61) Callaghan, P. T. *Principles of Nuclear Magnetic Resonance Microscopy*; Oxford University Press: Oxford, 1991.

(62) It may also be possible to reduce the effects of sample heating by reducing the power and/or duration of decoupling. However, because the onset of convection currents depends on the specific sample properties, the use of a double-stimulated echo may be preferred.

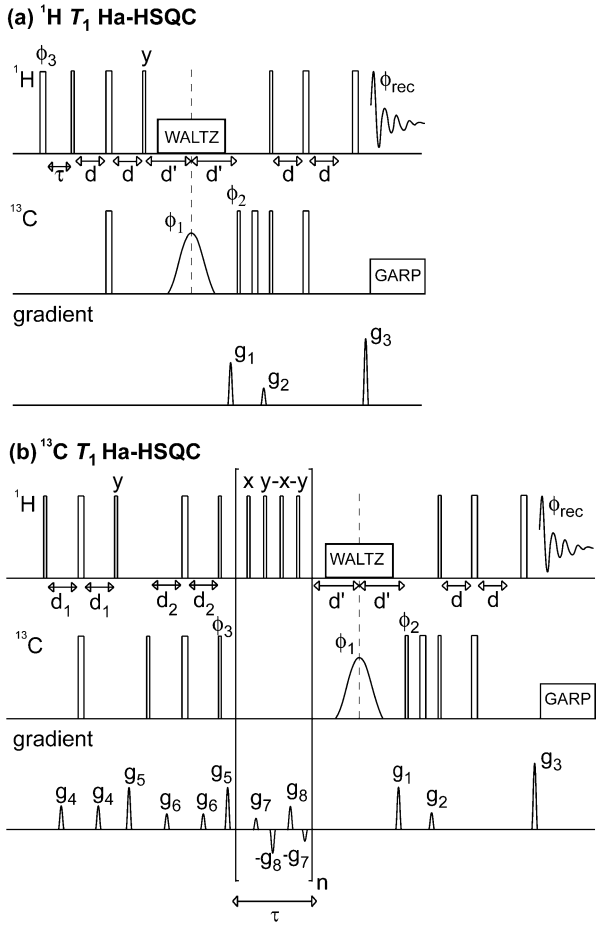

Figure 7. Schematic diagrams of Hadamard-encoded pulse sequences for the measurement of longitudinal spin−lattice (T_1) relaxation processes: (a) inversion recovery experiment with Ha-HSQC detection for the determination of ^{1}H T_1 relaxation times, and (b) experiment to determine ^{13}C T_1 relaxation times. The variable relaxation delay is abbreviated as τ, and in the refocused INEPT block of the ^{13}C T_1 Ha-HSQC experiment, d_1 was set to $1/(4J_{CH})$ and d_2 to $1/(8J_{CH})$. All phases are x unless otherwise specified. The following phase cycles were employed: (a) ^{1}H T_1 Ha-HSQC: $\phi_1 = (x)_4, (-x)_4$; $\phi_2 = x, -x$; $\phi_3 = (x)_2, (-x)_2$; $\phi_{rec} = (x, -x)_2, (-x, x)_2$; (b) ^{13}C T_1 Ha-HSQC: $\phi_1 = (x)_4, (-x)_4$; $\phi_2 = x, -x$; $\phi_3 = (y)_2, (-y)_2$; $\phi_{rec} = x, -x, -x, x, -x, x, x, -x$. The following gradient strengths were used in the different experiments: (a) ^{1}H T_1 Ha-HSQC: spoil gradient $g_1 = 1.25$ ms at 4.35 G/mm, encoding gradient $g_2 = 1.00$ ms at 6.52 G/mm, decoding gradient $g_3 = 1.00$ ms at 1.63 G/mm ($g_2/g_3 = 4{:}1$). (b) ^{13}C T_1 Ha-HSQC: g_1, g_2, g_3 as for ^{1}H T_1 Ha-HSQC, spoil gradients $g_4 = 0.9$ ms at 2.00 G/mm, $g_5 = 2.0$ ms at 4.00 G/mm, $g_6 = 0.7$ ms at 1.90 G/mm, $g_7 = 0.5$ ms at 0.50 G/mm, and $g_8 = 0.5$ ms at 1.00 G/mm.

as well as ethanol and glycerol, which differ by only 28%, to be determined despite their overlapping 1D ^{1}H spectra. If, despite the enhanced spectral resolution provided by the ^{1}H{^{13}C} HSQC or Hadamard-encoded experiments, one or more of the decays do not display monoexponential behavior, the number of components may still be reduced, making the application of postacquisition processing techniques more straightforward and robust.

Hadamard-Encoded, ^{1}H{^{13}C}-Resolved Spin-Relaxation Measurements. Analogous to the diffusion measurements above, Hadamard encoding can similarly yield enhanced temporal resolution of nuclear spin-relaxation times for mixtures with strongly overlapping signals in their 1D NMR spectra. The basic Ha-HSQC pulse sequence can be modified to yield Hadamard-encoded ^{1}H{^{13}C}-resolved experiments for the measurement of ^{1}H and ^{13}C longitudinal spin−lattice relaxation (T_1) times, as shown in Figure 7a and b, respectively, as well as for the measurement of ^{1}H and ^{13}C transverse spin−spin relaxation (T_2) times, as shown in Figure 8a and b. The inclusion of a Hadamard-encoded heteronuclear correlation block in pulse sequences for the measurement of ^{1}H relaxation rates is conceptually identical to the modification of the PG-STE and PG-DSTE sequences discussed above. Specifically, the hetero-

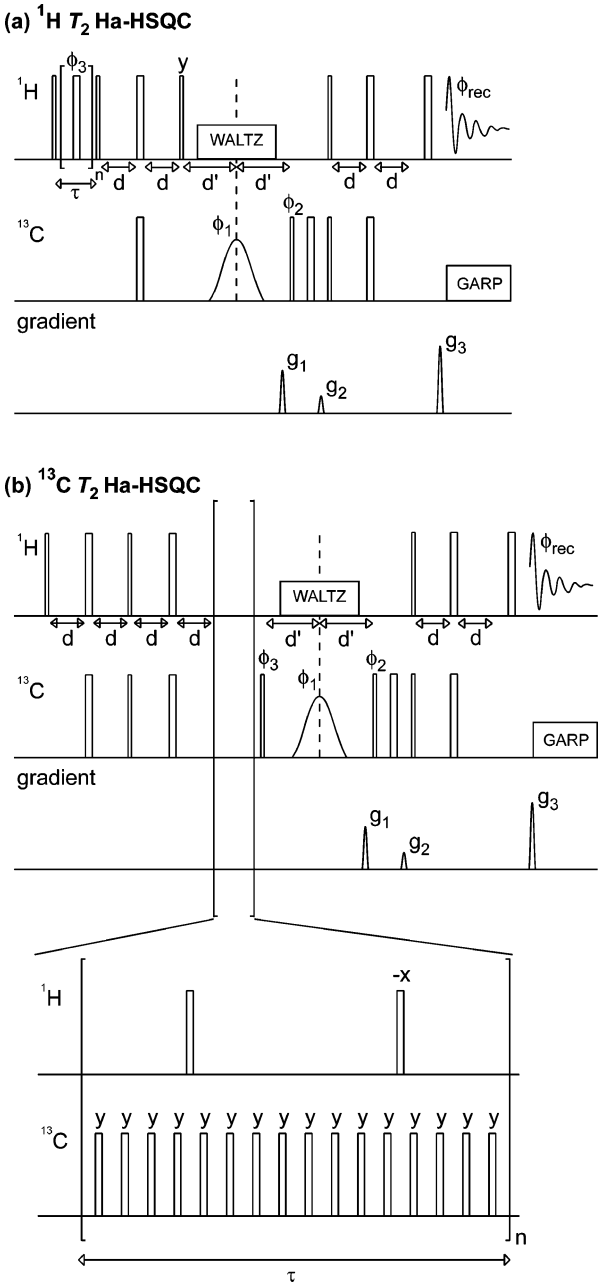

Figure 8. Schematic diagrams of Hadamard-encoded pulse sequences for the measurement of transverse spin−spin (T_2) relaxation processes for (a) ^{1}H and (b) ^{13}C. The variable relaxation time is abbreviated as τ and, for the ^{13}C T_2 Ha-HSQC experiment, ^{13}C refocusing pulses during the CPMG period were separated by $2\tau = 900$ μs. In addition, ^{1}H π-pulses were applied every 7.20 ms to remove cross-correlation effects. All phases are x unless otherwise specified. The following phase cycles were employed: (a) ^{1}H T_2 Ha-HSQC: $\phi_1 = (x)_4, (-x)_4$; $\phi_2 = x, -x$; $\phi_3 = (-y)_2, (y)_2$; $\phi_{rec} = (x, -x)_2, (-x, x)_2$; (b) ^{13}C T_2 Ha-HSQC: $\phi_1 = (x)_4, (-x)_4$; $\phi_2 = x, -x$; $\phi_3 = (x)_2, (-x)_2$; $\phi_{rec} = (x, -x)_2, (-x, x)_2$. The following gradient strengths were used in both experiments: spoil gradient $g_1 = 1.25$ ms at 4.35 G/mm, encoding gradient $g_2 = 1.00$ ms at 6.52 G/mm, and decoding gradient $g_3 = 1.00$ ms at 1.63 G/mm ($g_2/g_3 = 4{:}1$).

nuclear Hadamard-encoding block is added after the relaxation delay. In this way, the attenuated ^{1}H intensity serves as the initial amplitude for an Ha-HSQC experiment.

The modification of pulse programs designed for the measurement of ^{13}C nuclear spin-relaxation rates is slightly more complicated, but it is of particular interest, because it provides information on the reorientation dynamics of C−H bonds and the molecular moieties with which they are associated.[63] The corresponding pulse sequences are adapted to include Hadamard encoding by storing the ^{13}C along the *z*-axis immediately following the relaxation period and then applying selective inversion pulses. In this way, Hadamard-encoding can be used to measure ^{13}C T_2 relaxation by adapting a CPMG-based pulse sequence using ^{1}H π pulses to suppress cross-correlation effects,[53,64] as shown in Figure 8b. As a second example, a recently published pulse sequence,[52] optimized for the measurement of T_1 relaxation times in AX_2 systems (such as $-\mathbf{C}H_2-$ groups), was modified to include Hadamard encoding, as shown in Figure 7b. In this pulse sequence, a refocused INEPT sequence followed by a ^{13}C $\pi/2$ pulse is used to generate S_z magnetization, which then relaxes during the following delay period τ. Unwanted spin terms are purged during this period through the application of gradient pulses (to destroy double-quantum terms arising from dipole−dipole cross-correlated relaxation) and the use of ^{1}H $\pi/2$ pulses of varying phases to convert undesired zero-quantum coherences to double-quantum coherences. After the relaxation delay, the remaining S_z magnetization is phase encoded according to the prescribed Hadamard scheme and transferred back to protons for detection.[65]

The suitability of the Hadamard-encoded ^{1}H{^{13}C}-resolved pulse sequences for the measurement of ^{13}C T_1 relaxation times is illustrated in Figure 9 for the same aqueous mixture of 5 wt % ethanol, 10 wt % glycerol, and 2 wt % poly(ethylene glycol) at 298 K used in the diffusion measurements described above. The ^{13}C spin−lattice relaxation times for the various ^{13}C moieties in this solution were determined using the ^{13}C-T_1-Ha-HSQC pulse sequence shown in Figure 7b, and all transient signal decays were observed to be monoexponential. Consistent with its lower molecular weight, ethanol exhibited the slowest ^{13}C relaxation behavior in solution, and the T_1 relaxation times were found to be 8.42 ± 0.09 s and 7.52 ± 0.07 s for the $-\mathbf{C}H_2$-OH and the $-\mathbf{C}H_3$ carbon atoms, respectively. Glycerol ^{13}C nuclei were found to relax more quickly, with the corresponding relaxation times determined to be 3.08 ± 0.04 s and 1.75 ± 0.04 s for the $-\mathbf{C}$HOH− and the $-\mathbf{C}H_2$OH carbon atoms, respectively. Consistent with its higher molecular weight, poly(ethylene glycol) showed the shortest ^{13}C T_1 relaxation time, 0.597 ± 0.009 s for the $-O\mathbf{C}H_2\mathbf{C}H_2-$ carbon moieties. The validity of the Hadamard T_1 pulse sequence was confirmed by comparison with T_1 values measured separately in standard direct ^{13}C excitation/detection experiments. For example, for an aqueous 10 wt % glycerol solution at 298 K, 1D direct excitation/detection ^{13}C inversion−recovery experiments yielded a T_1 relaxation time of 2.03 ± 0.04 s for the $-\mathbf{C}H_2$OH ^{13}C glycerol moieties. This compares well with the relaxation time of 1.96 ± 0.06 s determined using the Hadamard-encoded experiment and is consistent with the lower viscosity of the glycerol solution compared to the PEG-containing mixture.

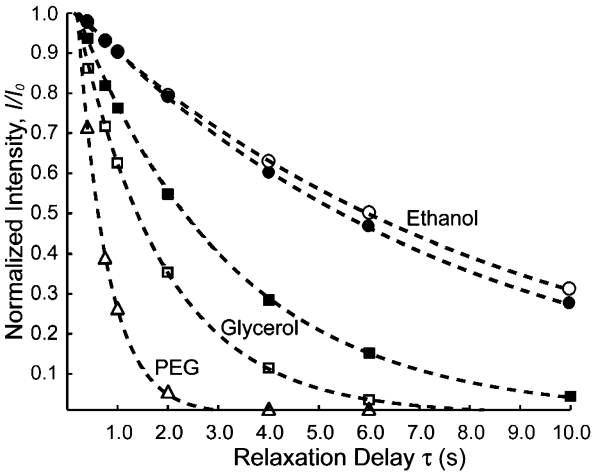

Figure 9. Transient ^{1}H-observed ^{1}H{^{13}C}-resolved signal-decay curves obtained for a mixture of 5 wt % ethanol, 10 wt % glycerol, and 2 wt % poly(ethylene glycol) in D_2O at 298 K using the Hadamard-encoded pulse sequence for the measurement of ^{13}C T_1 relaxation times [Figure 7b]. Data are shown for the ethanol $-\mathbf{C}H_3$ (●) and $-\mathbf{C}H_2$OH (○), the glycerol $-\mathbf{C}$HOH− (■) and $-\mathbf{C}H_2$OH (□), as well as the poly(ethylene glycol) $-O\mathbf{C}H_2\mathbf{C}H_2-$ (△) carbon moieties. All observed decays were well fitted with single exponential decays, which are shown as dashed lines.

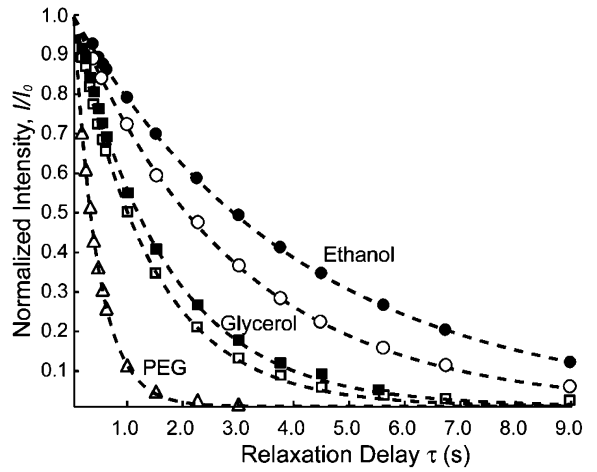

Figure 10. Transient ^{1}H-observed, ^{1}H {^{13}C}-resolved signal-decay curves obtained for a mixture of 5 wt % ethanol, 10 wt % glycerol, and 2 wt % poly(ethylene glycol) in D_2O at 298 K using the Hadamard-encoded pulse sequence for the measurement of ^{1}H T_2 relaxation times [Figure 8a]. Data are shown for the ethanol $-\mathbf{C}H_3$ (●) and $-\mathbf{C}H_2$OH (○), glycerol $-\mathbf{C}$HOH− (■) and $-\mathbf{C}H_2$OH (□), as well as the poly(ethylene glycol) $-O\mathbf{C}H_2\mathbf{C}H_2-$ (△) proton moieties. All observed decays were well fitted with single exponential decays, which are shown as dashed lines.

For the measurement of ^{1}H relaxation times, the first $\pi/2$ pulse of the Ha-HSQC pulse sequence [Figure 2a] is replaced with the corresponding spin-relaxation pulse sequence element, as shown in Figure 7a for longitudinal spin−lattice (T_1) or in Figure 8a for transverse spin−spin (T_2) relaxation time experiments. The results obtained using the Hadamard-encoded ^{1}H{^{13}C}-resolved pulse sequences for the measurement of ^{1}H T_2 relaxation times are shown in Figure 10 for the same aqueous mixture of 5 wt % ethanol, 10 wt % glycerol, and 2 wt % poly(ethylene glycol) at 298 K used in the diffusion and ^{13}C T_1

(63) Cavanagh, J.; Fairbrother, W. J.; Palmer, A. G.; Skelton, N. J. *Protein NMR Spectroscopy: Principles and Practice*; Academic Press: San Diego, CA, 1996.
(64) Palmer, A. G.; Skelton, N. J.; Chazin, W. J.; Wright, P. E.; Rance, M. *Mol. Phys.* **1992**, *75*, 699−711.
(65) To keep the pulse sequence as simple as possible a regular INEPT back-transfer was used, though a refocused INEPT step could be used to further improve the sensitivity of the experiment.

measurements described above. The transient signal decays obtained using the pulse sequence shown in Figure 8a were all observed to be monoexponential, and the corresponding time constants were determined from the respective and accompanying monoexponential fits. The $-C\mathbf{H}_3$ and $-C\mathbf{H}_2OH$ ethanol moieties showed the longest ^1H T_2 relaxation times, 4.13 ± 0.04 s and 2.92 ± 0.05 s, respectively, consistent with the small molecular hydrodynamic radius of ethanol and its correspondingly short rotational correlation time in aqueous solution. The different relaxation times for the two ethanol moieties reflect their different interactions with other molecules in solution, particularly water.[66] The $-C\mathbf{H}OH-$ and the $-C\mathbf{H}_2OH$ glycerol moieties relaxed more rapidly, exhibiting ^1H T_2 relaxation times of 1.66 ± 0.04 s and 1.40 ± 0.02 s, respectively. Consistent with expectations, the shortest ^1H T_2 relaxation time was observed for the largest molecular species in the solution, poly(ethylene glycol), whose $-OC\mathbf{H}_2C\mathbf{H}_2-$ moieties were measured to have T_2 values of 0.43 ± 0.01 s. The validity of the ^1H T_2 Ha-HSQC relaxation results was confirmed by comparing the ^1H T_2 relaxation times obtained for an aqueous 10 wt % glycerol solution at 298 K from the Hadamard-encoded experiment with those measured using a conventional ^1H T_2 pulse sequence in the absence of spectral overlap. The ^1H T_2 relaxation time of 1.063 ± 0.003 s obtained for the $-C\mathbf{H}OH-$ moieties measured with the conventional T_2 pulse sequence is in good agreement with the value of 1.069 ± 0.008 s obtained by using the Hadamard-encoded sequence in Figure 8a.

There are several complicating factors that may need to be taken into account when applying pulse sequences for measuring Hadamard-encoded $^1H\{^{13}C\}$-resolved nuclear spin-relaxation times, especially for ^{13}C. For example, cross-correlation effects involving different nuclear spin-relaxation pathways, such as between dipole−dipole interactions or between dipolar and chemical-shift-anisotropy interactions, may obscure the information being sought.[67−69] Through the use of specially designed pulse sequences, it is possible to suppress most of these unwanted competing relaxation pathways.[53,64,70−73] However, the transfer of magnetization between different nuclei using cross-polarization techniques or indirect (^1H) detection requires that several factors be taken into account.[74−76] For example, care must be taken that the magnetization generated during the preparation period corresponds to the desired initial condition for the relaxation process under investigation. To measure the decay of S_x or S_y coherences; for example, one needs to employ a refocused INEPT sequence, while for S_z the refocused INEPT sequence needs to be followed by an additional $\pi/2$ pulse. HSQC-resolved spin-relaxation measurements are commonly used in protein science, and a number of heteronuclear pulse sequences have been developed that minimize these interfering effects. As demonstrated here for the measurement of ^1H and ^{13}C T_1 and T_2 spin relaxation, such pulse sequences are readily adapted to include Hadamard encoding. These examples should also serve as a basis for adapting newly emerging pulse sequences, such as those for measuring off-resonance $T_{1\rho}$ relaxation processes, to include a Hadamard component for improved temporal resolution and faster acquisition times.[77,78]

Thus, Hadamard encoding can be used determine accurately and rapidly ^{13}C and ^1H T_1 and T_2 relaxation times in complex solutions, such as the aqueous mixture of ethanol, glycerol, and poly(ethylene glycol) examined here. Moreover, the Hadamard measurements were found to be substantially faster than the corresponding HSQC-resolved experiments by a factor of 8, similar to the diffusion measurements and consistent with the estimated time savings discussed previously. The four pulse sequences shown in Figures 7 and 8 represent a convenient set of experiments for determining T_1 and T_2 relaxation times for both ^1H and ^{13}C, as well as serving as templates for adapting further spin-relaxation pulse sequences to include Hadamard encoding.

Ha-PG-DSTE Measurements of Guest−Host Interactions in Micellar Solutions. To demonstrate the applicability of the methods described above to more complicated solution mixtures, the Ha-PG-DSTE pulse sequence was used to investigate the interactions of organic guest species that associate with self-assembling host block copolymer species in aqueous solution. The solubilization, binding, or encapsulation of organic dye or drug molecules within block-copolymer host systems is important in a wide variety of applications, including drug delivery and optical materials processing. As a representative heterogeneous system, an aqueous solution containing water-soluble *tetra*(4-sulfonatophenyl)porphyrin ($TPPS_4$) dye species and amphiphilic poly(ethylene oxide)−poly(propylene oxide)−poly(ethylene oxide) (PEO−PPO−PEO) triblock copolymer species was investigated. This system is closely related to precursor mixtures for preparing mesostructured inorganic−organic hybrid films with optical limiting properties.[79]

Full quasi-3D $^1H\{^{13}C\}$ HSQC diffusion measurements were recently used to demonstrate that selective and strongly temperature-dependent interactions in the $EO_{20}PO_{70}EO_{20}/TPPS_4$ system have a significant effect on the aggregation behavior of the block-copolymer host.[21] As shown in Figure 11a, the acquisition of a full $^1H\{^{13}C\}$ HSQC spectrum was necessary to clearly resolve and assign the different and otherwise overlapping PEO and PPO resonances of the triblock-copolymer species for an experiment conducted at 45 °C (318 K). Furthermore quasi-3D $^1H\{^{13}C\}$ HSQC-PG-DSTE experiments were necessary to assign unambiguously the PEO[80] signals to contributions from micellar aggregates (peak 1) and soluble unimers (peak 2), which displayed stronger interactions with the aromatic $TPPS_4$ dye species. As shown in Figure 11b, the signal associated with peak 1 (◇) decays monoexponentially and more

(66) Sacco, A.; De Cillis, F. M.; Holz, M. *J. Chem. Soc., Faraday Trans.* **1998**, *94*, 2089−2092.
(67) Werbelow, L. G.; Grante, D. M. *Adv. Magn. Reson.* **1977**, *9*, 189−299.
(68) Vold, R. L.; Vold, R. R. *Prog. Nucl. Magn. Reson. Spectrosc.* **1978**, *12*, 79−133.
(69) Solomon, I. *Phys. Rev.* **1955**, *99*, 559−565.
(70) Peng, J. W.; Wagner, G. *J. Magn. Reson.* **1992**, *98*, 308−332.
(71) Goldman, M. *J. Magn. Reson.* **1984**, *60*, 437−452.
(72) Mayne, C. L.; Grant, D. M.; Alderman, D. W. *J. Chem. Phys.* **1976**, *65*, 1684−1695.
(73) Fischer, M. W. F.; Majumdar, A.; Zuiderweg, E. R. P. *Prog. Nucl. Magn. Reson. Spectrosc.* **1998**, *33*, 207−272.
(74) Kay, L. E.; Bull, T. E.; Nicholson, L. K.; Griesinger, C.; Schwalbe, H.; Bax, A.; Torchia, D. A. *J. Magn. Reson.* **1992**, *100*, 538−558.
(75) Bodenhausen, G.; Ruben, D. J. *Chem. Phys. Lett.* **1980**, *69*, 185−189.
(76) Palmer, A. G.; Wright, P. E.; Rance, M. *Chem. Phys. Lett.* **1991**, *185*, 41−46.
(77) Korzhnev, D. M.; Orekhov, V. Y.; Kay, L. E. *J. Am. Chem. Soc.* **2005**, *127*, 713−721.
(78) Korzhnev, D. M.; Orekhov, V. Y.; Dahlquist, F. W.; Kay, L. E. *J. Biomol. NMR* **2003**, *26*, 39−48.
(79) Melosh, N. A.; Steinbeck, C. A.; Scott, B. J.; Hayward, R. C.; Davidson, P.; Stucky, G. D.; Chmelka, B. F. *J. Phys. Chem. B* **2004**, *108*, 11909−11914.
(80) In the block-copolymer literature the designation poly(ethylene oxide) (PEO) is often used in favor of poly(ethylene glycol) (PEG) even for low molecular weight $(-OCH_2CH_2-)_n$ polymers.

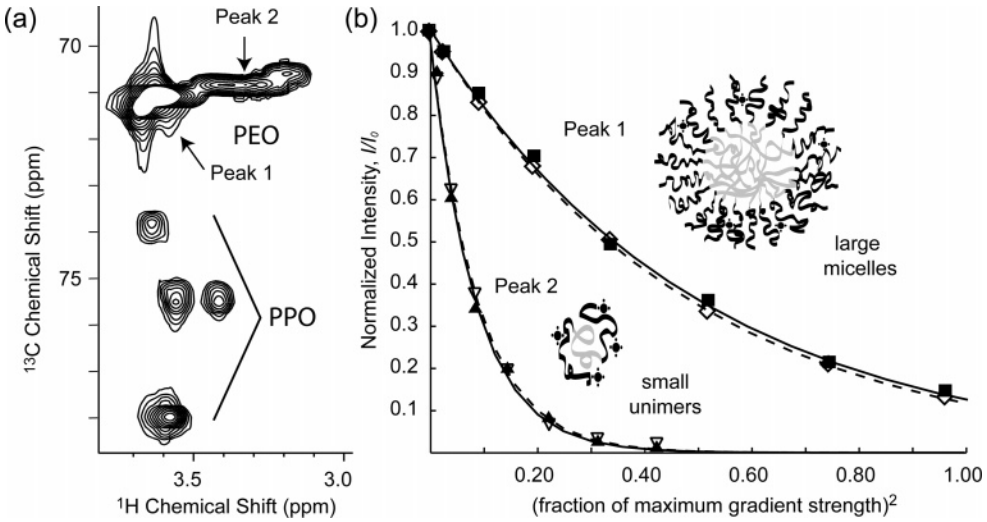

Figure 11. (a) 2D ^{1}H{^{13}C} HSQC spectrum showing resolved PEO and PPO resonances for an aqueous mixture (pH = 11) of 10 mM (ethylene oxide)$_{20}$-(propylene oxide)$_{70}$(ethylene oxide)$_{20}$ and 10 mM *tetra*(4-sulfonatophenyl)porphyrin dye species at 45 °C (318 K). (b) Comparison of diffusion data obtained from a full quasi-3D HSQC-PG-DSTE experiment and a corresponding Ha-PG-DSTE experiment. The experimentally observed decay curves show that the results from the Ha-PG-DSTE experiment (▲, ■, solid fit lines) agree very well with those obtained from the quasi-3D HSQC-PG-DSTE experiments (▽, ◇, dashed fit lines).

slowly than that associated with peak 2 (▽); the fits to each decay (shown as dotted lines) lead to self-diffusion coefficients of $D^{PEO}_{peak1}/D_{water} = 0.010 \pm 0.001$ and $D^{PEO}_{peak2}/D_{water} = 0.050 \pm 0.001$, corresponding to micelle and unimer species, respectively. The acquisition of such quasi-3D spectra, however, is time-intensive (~16 h/spectrum), so that establishing temperature-dependent block-copolymer/dye interactions and their influences on solution phase behavior required a total measurement time of approximately 1 week.[21] By comparison, the use of the Ha-PG-DSTE sequence allowed the same information to be acquired in less than $^{1}/_{10}$ of the time, ~1.5 h/spectrum. As shown in Figure 11b, fits (solid lines) to the signal decays measured for peaks 1 (■) and 2 (▲) using the Hadamard sequence lead to self-diffusion coefficients for the micelle ($D^{PEO}_{peak1}/D_{water} = 0.010 \pm 0.001$) and unimer ($D^{PEO}_{peak2}/D_{water} = 0.052 \pm 0.002$) species that are identical (within experimental uncertainties) to the quasi-3D results. Hadamard-encoded ^{1}H {^{13}C}-resolved diffusion (and relaxation) measurements are thus versatile and a general means for analyzing dynamic processes not only for chemically similar mixtures but also for investigating interaction processes in more complex heterogeneous solutions, in particular technologically important mixtures with self-assembling components.

Conclusions

The incorporation of Hadamard encoding in ^{1}H{^{13}C} NMR pulse sequences for the determination of molecular self-diffusion coefficients and nuclear spin-relaxation times allows for the time-efficient spectroscopic discrimination of similar exponential signal decays. The resulting resolved signal decay curves can be used with existing postacquisition analysis techniques to increase significantly the resolution of similar or, in the case of complete spectral resolution, identical decay constants. For example, diffusion coefficients of ethanol and glycerol in aqueous solutions differing by only 28% could be determined without difficulty, representing a significant improvement over conventional 1D ^{1}H PGSE self-diffusion experiments, which cannot distinguish such similar values. Furthermore, Hadamard-encoded experiments provide substantially greater sensitivity than full 2D experiments for the same measuring time. For a given signal-to-noise ratio, the time savings of Hadamard-encoded diffusion or spin-relaxation measurements are significant (approximately an order of magnitude). The resulting reduction in overall measuring times allows more sensitive and better resolved measurements of dynamic molecular processes than previously possible. This is expected to be useful for monitoring the dynamic properties of slowly evolving complex fluid systems, e.g., the changing aggregation states of molecular species (reflected as changes in their diffusion coefficients). The incorporation of other Hadamard-encoded homo- or heteronuclear correlation experiments into pulse sequences for the measurement of transient signal decay constants is expected to be general and should allow overlapping resonances and associated signal decays to be resolved in a variety of different molecular systems. This includes extensions to nuclei other than ^{1}H and ^{13}C, such as ^{15}N, ^{29}Si, ^{31}P, along with quadrupolar nuclei, with application to the characterization and dynamic analyses of complicated solution mixtures.

Acknowledgment. The authors thank Dr. Niklas Hedin and Dr. Peter Bendel for helpful discussions. This work was supported in part by the U.S. National Science Foundation Division of Materials Research under Award DMR-02-33728 and through the MRSEC program via the UCSB Materials Research Laboratory under Award DMR-00-80034 and by the USARO through the Institute for Collaborative Biotechnologies.

JA0439064